Comparing numerical solutions for the propagation of brittle fractures based on local energy minimization with classical fracture mechanics results.

Maurizio Angelillo[1], Enrico Babilio[2]
[1]*Department of Civil Engineering, University of Salerno, Italy*
E-mail: mangelillo@unisa.it

[2]*Department of Structures and Mathematical Methods in Architecture, University of Neaples Federico II, Italy*
E-mail: enrico.babilio@unina.it

Keywords: Calculus of Variations, Fracture Mechanics, Numerical descent methods.

SUMMARY. Our research group at the University of Salerno is developing since a decade a computer code for the minimization of complex functionals, based on descent methods. Recent applications have been concerned with masonry–like materials, Folding of thin walled tubes and Fracture of two–dimensional brittle solids. The present study is based on the variational model for quasi–static crack propagation proposed by Francfort and Marigo. Essentially their model extends the classical Griffith's energy criterion with a unilateral global minimality property and an energy balance condition. This is a typical problem of minimization with free discontinuities for which the main unknown is the jump set Γ. The variational model of Francfort and Marigo for crack propagation and initiation has been recently implemented in our developing code for elastic–brittle fracture. Actually our approach lean on local rather than on global minimization but, in the present study, we restrict to cases for which local and global minimization are expected to give the same answers. With our computer program, restricted to small strain plane elasticity and based on classical triangular finite elements, approximate solutions are searched by minimizing (locally) the potential energy with a descent method. The potential energy is the sum of the bulk strain energy defined over the triangles and the surface fracture energy defined over the skeleton of the triangulation. The first, natural, variables we consider are the node displacements (possibly discontinuous across triangle boundaries). The second variables we consider are the node positions in the reference configuration. By considering these positions variable and part of the minimization strategy, we allow for the skeleton of the mesh to adapt to optimal fracture patterns. In the present work our computer model is validated by comparing our results with the predictions in terms of energy levels, stress intensity factor and crack orientation, of Linear Elastic Fracture Mechanics and the criterion of maximum Energy Release Rate for several Mode I, Mode II load combinations.

1 INTRODUCTION

The finite element method is widely employed in fracture mechanics modelling and many numerical models for crack discontinuity simulations in brittle materials, based on different finite element approaches, can be found in the literature.

They can be mainly classified into *smeared* and *discrete* crack approaches. In the smeared models, the crack is smeared out into the material in a continuous fashion so that this kind of models can be managed numerically using conventional C^0 elements. Smeared cracks introduce softening that produces strain localization into bands of zero width. This kind of localization is physically incorrect and leads to numerically ill posed equations since the energy dissipation vanishes and the

solution is mesh dependent. In order to prevent this spurious localization one needs to introduce an internal length scale as a material parameter.

In the discrete approaches, the softening behaviour resulting from the fracture process is described by using a traction- displacement relation on the discontinuity surface (along a line in 2D), whilst the bulk of the material is characterized by a stress-strain relationship. In energy terms there is an interface energy density controlling the traction-displacement relation on the interface and a bulk elastic energy density. For the numerical implementation, special element type and formulations are necessary. Many different element formulations can be found in the literature to simulate the nucleation and growth of discontinuities and cracks, in some of them the finite elements are continuous and the discontinuity can occur inside the elements (see [1] and [2]).

In our 2D approach we consider special gap elements of zero thickness placed along the edges of continuous elements. Being the crack location and orientation not known in advance, we adopt finite elements based on variable meshes which give to the skeleton of the mesh the ability to adapt to optimal fracture patterns (see [3, 4, 5, 6, 7, 8]). From the mathematical point of view, our numerical implementation of quasi-static brittle fracture is based on the variational formulation of Francfort and Marigo [9] the main difference being the fact that we rely on local rather that on global minimization. Propagation of fracture is obtained by minimizing in a step by step process a form of energy that is the sum of bulk and interface terms. Scope of the present work is to present some numerical experiments devoted to the comparison of our results with analytical solutions for crack propagation based on classical fracture mechanics.

2 NUMERICAL STRATEGY

The approach we are dealing with is reported in details in [8] and it will be briefly summarized for the reader's convenience.

2.1 Preliminaries

Consider a two–dimensional body $\mathcal{B}$ occupying in the original configuration a bounded plane domain Ω and undergoing small deformations. Let

$$\boldsymbol{\varepsilon} = \frac{1}{2}(\nabla \mathbf{u} + \nabla \mathbf{u}^T) \tag{1}$$

be the infinitesimal strain tensor, being $\mathbf{u}$ the displacement field defined over Ω. The boundary $\partial\Omega$ is partitioned into Dirichlet part $\partial\Omega_D$ and Neumann part $\partial\Omega_N$, where displacements $\bar{\mathbf{u}}$ and tractions $\bar{\mathbf{p}}$ are given respectively. We admit that $\mathbf{u}$ may be discontinuous on a set $\Gamma \subset \Omega$ assumed to belong to an admissible set of cracks

$$\mathbb{\Gamma} = \{\Gamma \subset \bar{\Omega} \setminus \partial\Omega_N, \text{ s. t. } \Gamma \text{ is closed}, \mathcal{H}^1(\Gamma) < \infty\} , \tag{2}$$

$\mathcal{H}^1$ being the one–dimensional Haussdorff measure.

The crack pattern Γ is the most relevant unknown in fracture problems and the theorems of Ambrosio [10], valid in particular for Griffith's type variational formulations based on global minimizers, ensure that Γ is sufficiently regular to be approximated by sets composed by regular arcs, such as edge elements, so that $\mathcal{H}^1(\Gamma)$ coincides with the usual arc length and unit normal $\mathbf{n}$ and tangent $\mathbf{t}$ exist a.e. along Γ.

The jump of $\mathbf{u}$, denoted by $[\![\mathbf{u}]\!] = \mathbf{u}^+ - \mathbf{u}^-$ and resolved into two components relative to $\mathbf{n},\ \mathbf{t}$

$$[\![\mathbf{u}]\!] = a\mathbf{n} + b\mathbf{t} , \tag{3}$$

is defined in such a way that if a is positive the corresponding points on the two opposite sides of the interface determine a vacancy.

Finally we assume

$$\mathbf{u} \in \mathrm{H}^1(\Omega \setminus \Gamma) \,. \tag{4}$$

2.2 Volume and surface energy densities

The material is assumed to be elastic and isotropic, that is characterized by the elastic energy density

$$\varphi(\boldsymbol{\varepsilon}) = \frac{1}{2}\Big(\lambda^\star(\mathrm{tr}\boldsymbol{\varepsilon})^2 + 2\mu\boldsymbol{\varepsilon}\cdot\boldsymbol{\varepsilon}\Big) \,, \tag{5}$$

defined over $\Omega \setminus \Gamma$, being $\lambda^\star$ and μ the elastic moduli for generalized plane stress.

To model brittle fracture, we introduce the interface energy density

$$\vartheta(a,b) = \begin{cases} 0, & a = 0,\ b = 0, \\ \gamma, & a > 0, \\ +\infty, & a < 0 \ \text{ or } \ a = 0,\ b \neq 0, \end{cases} \tag{6}$$

where γ is the surface energy density of the material.

2.3 The Boundary Value Problem

We consider quasi–static BVP's. A typical example is represented by the plane strip of heigth H and width B shown in Figure 3 to which we refer for notations. On $\partial\Omega_N,\ \bar{\mathbf{p}} = 0$ and on $\partial\Omega_D = \Sigma^0 \cup \Sigma^H$ a combination of relative displacements $\bar{\mathbf{u}}$ is given. We assume $\bar{\mathbf{u}}$ to be time dependent and of the form

$$\bar{\mathbf{u}}_{\Sigma^0} = \mathbf{U}_0(\tau),\ \bar{\mathbf{u}}_{\Sigma^H} = \mathbf{U}_H(\tau) \,. \tag{7}$$

At any step of the loading process we seek equilibrium states of the strip as stationary points of the functional

$$F(\Gamma;\mathbf{u}) = \int\limits_{\Omega\setminus\Gamma} \varphi(\boldsymbol{\varepsilon})d\mathbf{x} + \int\limits_{\Gamma} \vartheta([\![\mathbf{u}]\!])ds \,, \tag{8}$$

under the condition (7). Actually, for any $\Gamma \in \mathbb{\Gamma}$, one could find the $\mathbf{u}$ corresponding to Γ by solving the problem

$$F^\circ = \min_{\substack{\mathbf{u}\in\mathrm{H}^1(\Omega\setminus\Gamma) \\ \mathbf{u}=\bar{\mathbf{u}} \text{ on } \partial\Omega_\mathrm{D}}} F(\Gamma;\mathbf{u}) \,. \tag{9}$$

2.4 Space discretization

To discretize the problem we split the domain Ω into triangles, as shown in Figure 3, and identify Γ with the skeleton of the triangulation. In order to duplicate nodes and edges of the skeleton of the mesh, we introduce special interface elements with zero thickness placed along the edges of the continuous elements.

2.5 Approximate surface energy density

In the numerical applications we approximate the equilibrium trajectory of the system by considering crack propagation as based on critical points of the energy. To get out of possible small energy wells, either numerical (due to the finite element mesh) or physical (due to fracture initiation), we adopt an approximate relaxed form of the surface energy density (6).

On introducing the limit tensile stress σ_0, the limit shear stress τ_0, the surface energy density γ, the shear stiffness k and the functions $\vartheta_1(a)$ and $\vartheta_2(b)$, depicted in Figure 1

$$\vartheta_1(a) = \gamma + \frac{2\gamma}{\pi - 2}\left(\mathrm{e}^{\frac{a\psi\sigma_0}{\gamma}} - 2\arctan\left[\mathrm{e}^{\frac{a\psi\sigma_0}{\gamma}}\right]\right) , \tag{10}$$

$$\vartheta_2(b) = \frac{2\tau_0}{k\pi^2}\left(k\pi b\arctan\left[\frac{k\pi b}{2\tau_0}\right] - \tau_0\log\left[1 + \left(\frac{k\pi b}{2\tau 0}\right)^2\right]\right) , \tag{11}$$

where

$$\psi = \frac{2-\pi}{\sqrt{2(5\sqrt{5}-11)}} , \tag{12}$$

the relaxed interface energy density is

$$\bar{\vartheta}(a,b) = \vartheta_1(a) + \mathrm{e}^{-\tau_0 a}\vartheta_2(b) . \tag{13}$$

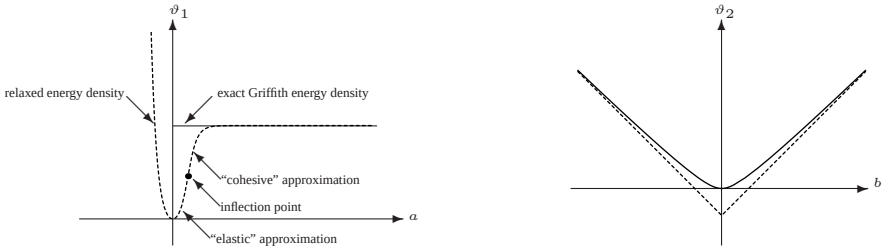

a. b.

Figure 1: The function $\vartheta_1(a)$ superimposed to the exact Griffith surface energy density and the function $\vartheta_2(b)$.

Notice that although the density (13) has a shape close to that of the approximate surface energy density defined in [8], the main difference between them is that all parameters in the function (13) have a clear physical meaning and no shape parameter is needed.

2.6 Descent minimization

The potential energy is the sum of the bulk elastic energy plus the interface energy where the densities (5) and (13) are defined on the continuous elements and on the special interface elements, respectively. At each step of the loading process, the search for the minimum proceeds through the nonlinear Polak–Ribière Conjugate Gradient Method, that is an iterative deterministic algorithms for finding local minima of multivariate functions whose arguments are continuous. Chosen a starting point P_0, in the first iteration the search direction is taken as the negative gradient of the objective function at P_0. Then the search directions are computed by Gram–Schmidt conjugation of the residuals. The method is implemented in the open source code *Surface Evolver* [11], a minimization tool originally designed to find minimal surfaces shaped by surface tension, such as foams, and substantially modified by the authors in order to adapt it to the purposes of the present study.

3 ANALYTICAL RESULTS

Path–independent integrals, derived from conservation laws, are used in physics to calculate the intensity of a singularity of a field quantity without knowing the exact shape of this field near the singularity. Rice [12] introduced path–independent integrals into fracture mechanics.

Consider a two–dimensional body of perimeter K with prescribed displacement on the Dirichlet part and tractions on the Neumann part of the boundary and a pre–existing crack and assume the coordinates are attached at the crack tip.

The potential energy Π of the body is given by

$$\Pi = \int\limits_{\Omega} w da - \int\limits_{\mathrm{K}} t_i u_i dS \, . \tag{14}$$

where $w = \int_0^{\varepsilon_{ij}} \sigma_{ij} d\varepsilon_{ij}$. Let us consider the tip of the crack underoing a virtual dispalcement by an infinitesimal distance dl oriented at an arbitrary angle α, so that the total energy release rate is

$$\frac{d\Pi}{dl} = \int\limits_{\Omega} \frac{dw}{dl} da - \int\limits_{\mathrm{K}} t_i \frac{du_i}{dl} dS \, . \tag{15}$$

After some calculations (see [12] and [13])

$$\frac{d\Pi}{dl} = -n_i J_i = -(J_1 \cos\alpha + J_2 \sin\alpha) \, . \tag{16}$$

where

$$J_i = \int\limits_{\mathrm{K}} w m_i - t_j \left(\frac{\partial u_j}{\partial x_i} \right) ds \, , \tag{17}$$

are the components of the J–vector, m_i are the components of the outward unit vector normal to the curve K, $n_1 = \cos\alpha$ and $n_2 = \sin\alpha$. J_1 is the "J–integral" as introduced by Rice [12] and it is path–independent, provided that the integral along the curve K surrounding the notch tip be evaluated in a contraclockwise sense starting from the lower flat notch surface to the upper flat surface, the enclosed area in the curve K be in equilibrium and the energy density w be a unique function of the strains.

On introducing the angle $\varphi = \arctan \frac{J_2}{J_1}$, from the equation (15) we get

$$-\frac{d\Pi}{dl} = \sqrt{J_1^2 + J_2^2} \cos(\varphi - \alpha) = G \, , \tag{18}$$

G being the rate of change of potential energy associated with crack advance introduced by Irwin [14]. The maximum rate is achieved for $\alpha = \varphi$

$$G_{\max} = \sqrt{J_1^2 + J_2^2} \, . \tag{19}$$

It follows that once $G_{\max} \geq G_c$, G_c being the material toughness, crack tip will advance along angle α.

Let assume that the loading applied at remote consists of a combination of horizontal and vertical loads $\bar{q}_1$ and $\bar{q}_2$ such that $\bar{q}_2 = \bar{q}_1 \tan\beta$, β being the load angle. The corresponding stress intensity factors K_I and K_{II} at the tip of the crack are of the order of $\bar{q}_2\sqrt{\pi a}$ and $\bar{q}_1\sqrt{\pi a}$, a being the crack length.

In case of plane stress, the components of the J–vector are

$$J_1 = \frac{K_I^2 + K_{II}^2}{E} \,, \qquad J_2 = -\frac{2K_I K_{II}}{E} \,, \tag{20}$$

where E is the Young modulus. The crack tip will advance along the angle

$$\alpha = -\arctan\left[\frac{2K_I K_{II}}{K_I^2 + K_{II}^2}\right] = -\arctan\left[\sin 2\beta\right] . \tag{21}$$

A plot of the crack angle α versus the load angle β is shown in Figure 2.

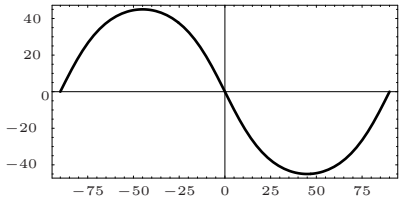

Figure 2: The crack angle α as a function of the load angle β

4 NUMERICAL RESULTS

As a numerical application we consider the benchmark example represented by the notched plane strip of heigth H and width B shown in Figure 3, to which we refer for notations.

On $\partial\Omega_N$, $\bar{\mathbf{p}} = 0$ and on $\partial\Omega_D = \Sigma^0 \cup \Sigma^H$ a combination of relative displacements $\bar{\mathbf{u}}$ of the form (7) is applied.

Though we could use the analytical solution of Section 3 as a qualitative guide, the quantitative results are in this case different since the specimen has a "finite size" and the displacement not the load is considered as the driving force.

We assume $\mathbf{U}_{\text{-}}(\tau) = S_{\text{-}}(\tau)\,\hat{\mathbf{e}}_1 + V_{\text{-}}(\tau)\,\hat{\mathbf{e}}_2 = S_{\text{-}}(\tau)(\hat{\mathbf{e}}_1 + \tan\beta\,\hat{\mathbf{e}}_2)$, where $\mathbf{U}_{\text{-}}$ is $\mathbf{U}_0$ or $\mathbf{U}_H$ and β is the angle in between the displacement direction and the horizontal unit vector $\hat{\mathbf{e}}_1$. Therefore here the angle β is the displacement angle rather than the load angle.

Geometrical and material constants of the specimen are reported in the Table 1.

Table 1: Geometrical and material constants of the specimen

Height	Length	Thickness	Young Modulus	Poisson ratio
H (cm)	L (cm)	t (cm)	E (Ncm^{-2})	ν
10.0	10.0	1.0	$3.0\ 10^5$	0.0

The results of the computations are shown in terms of J_i components and in terms of crack pattern. In order to evaluate the J–vector the contour integral (17) should be calculated but, unfortunately, it is quite unfavourable in a finite element model as coordinates and displacements refer to nodal points and stress fields are generally discontinuous over element boundaries. Hence, a domain integral method is commonly used instead. Applying the divergence theorem, the contour integral (17) can be reformulated as an area integral in two dimensions, over a finite domain Ω_0 surrounding the crack front. The J–integral is associated with a fictitious small crack advance δl,

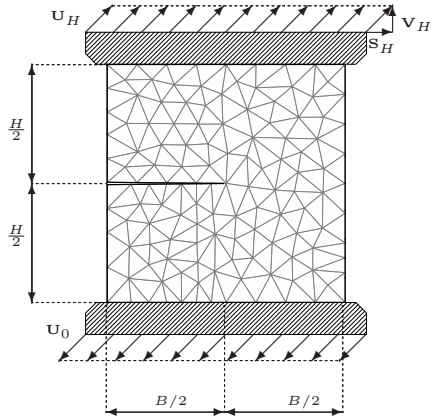

Figure 3: The specimen: boundary conditions and initial mesh

giving all nodes on and inside a contour C_0 (the internal boundary of Ω_0) the displacement δl and leaving fixed at their original position all nodes on and outside a contour C_1 (the external boundary of Ω_0), completely surrounding C_0

$$J\delta l = \int\limits_{\Omega_0} \left(\sigma_{ij} \frac{\partial u_i}{\partial x_k} \frac{\partial \delta u_k}{\partial x_j} - w \frac{\partial \delta u_k}{\partial x_k} \right) da \tag{22}$$

where δu_k is the shift of the crack front coordinates (i.e. the points on and inside C_0).

The method, suggested by Parks [15] and known as "Virtual Crack Extension" (*VCE*), is quite robust in the sense that accurate values are obtained even with quite coarse meshes.

The component J_1 (respectively J_2) of the J–vector is computed by choosing the *VCE* parallel (perpendicular) to the crack plane, i.e. δa has the direction of x_1 (x_2), $\delta a = \delta x_1$ ($\delta a = \delta x_2$).

In what follows, we consider Ω_0 as a one–element crown, as shown in Figure 4 and employ constant strain finite elements, so that we can rewrite the equation (22) as

$$J_k \delta u_k = \sum_{el=1}^{N(\Omega_0)} \left(\sigma_{ij}^{(el)} \frac{\partial u_i}{\partial x_k}^{(el)} \frac{\partial \delta u_k}{\partial x_j}^{(el)} - \frac{1}{2} \sigma_{ij}^{(el)} \varepsilon_{ij}^{(el)} \frac{\partial \delta u_k}{\partial x_k}^{(el)} \right) A r^{(el)} \tag{23}$$

where $N(\Omega_0)$ is the number of triangles contained in the crown (see Figure 4). The results reported in Table 2 in terms of the crack initiation angles agree sharply with the predictions of classical Fracture Mechanics. In Figure 6 deformed elastic and fractured configurations are shown.

5 CONCLUSIONS

In this paper some benchmark problems under Mode I, Mode II load combinations are considered. The scope is to validate a computer model by comparing our results with the predictions of Linear Elastic Fracture Mechanics. The computer approach belongs to the family of discrete crack models. Special interface elements with zero thickness placed along the edges of continuous

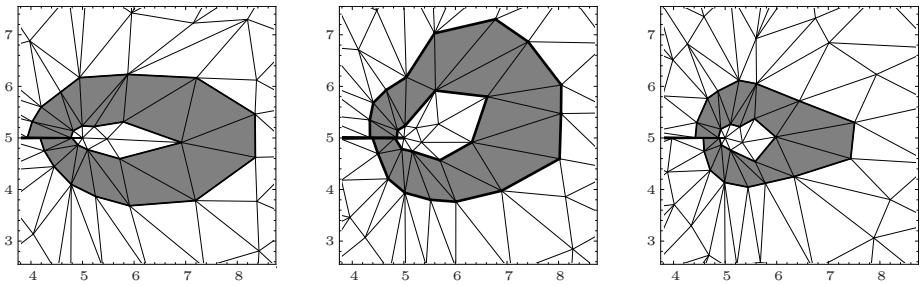

Figure 4: The integration domain Ω_0 (shaded area).

Table 2: Results for several displacement angles

displacement angle β	J_1 Ncm^{-1}	J_2 Ncm^{-1}	crack angle α Classical Fracture Mechanics	crack angle α Numerical Experiments
$0°$	0.4445	0.0247	$-\ 3.1762°$	$-\ 2.7787°$
$45°$	1.9248	1.1311	$-30.4395°$	$-30.4583°$
$90°$	1.4964	0.0080	$-\ 0.3065°$	$-\ 0.4279°$

triangular elements are considered and, since the crack location and orientation is not known in advance, a variable mesh is adopted in order to allow for the skeleton of the mesh to adapt to optimal fracture patterns. Special attention is paid to the numerical implementation concerning crack path irreversibility. In particular if a piece of crack opens up at a certain step, it is maintained at any successive step. The proposed method needs no assumptions on the crack geometry in advance. Numerical tests of a notched specimen for different applied boundary conditions are analyzed. The results are sufficiently satisfactory for the three different cases studied. The discontinuity can run arbitrarily through the finite element mesh as shown in the examples and all the crack initiation angles are found to agree sharply with the predictions of classical Fracture Mechanics.

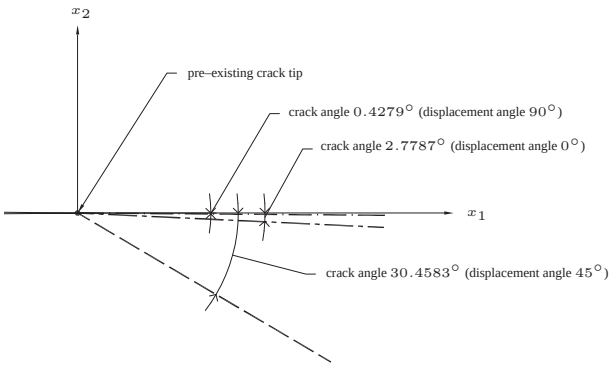

Figure 5: Superimposition of the results of the numerical experiments in terms of crack angles.

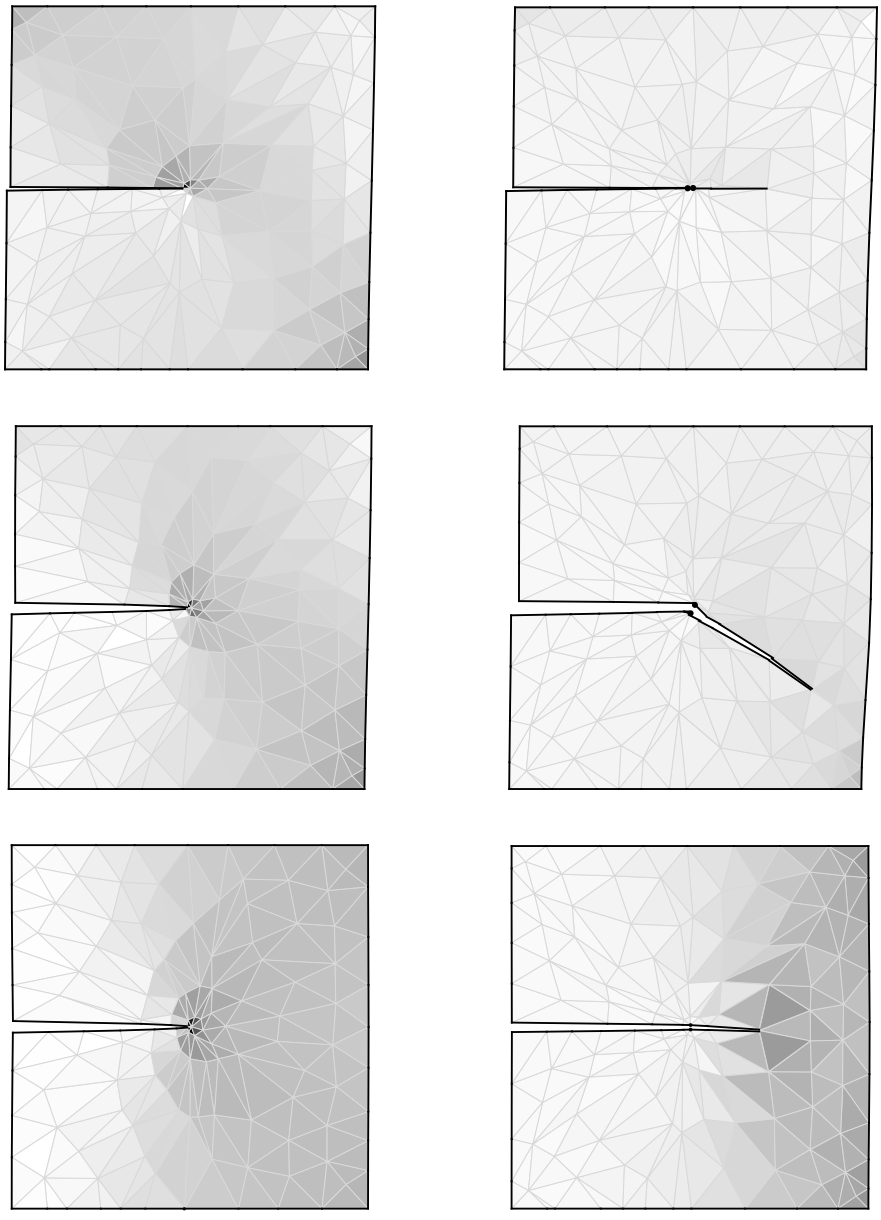

Elastic solution Fractured solution

Figure 6: Results of numerical tests for three displacement boundary conditions. From top to bottom: $\beta = 0°$, $\beta = 45°$, $\beta = 90°$.

References

[1] Belytschko, T., Fish, J. and Engelmann, B. E., "A finite element with embedded localization zones," *Comp. Meth. Appl. Mech. Eng.*, **70** (1), 59–89 (1988).

[2] Negri, M., "A discontinuous finite element approach for the approximation of free discontinuity problems," *Adv. Math. Sci. Appl.*, **15**, 283–306 (2005).

[3] Angelillo, M., Babilio, E. and Fortunato, A., "Numerical experiments on fracture of elastic solids through energy minimization," *Proc. of 2nd CanCNSM*, Vancouver, Canada, June 19-23, 2002, E. M. Croitoro ed., 181–186 (2002).

[4] Angelillo, M., Babilio, E. and Fortunato, A., "A numerical method for fracture of rods," In *Mechanical Modelling and Computational Issues in Civil Engineering*, Lecture Notes in Applied and Computational Mechanics, Volume 23, Springer-Verlag, Berlin, M. Fremond and F. Maceri eds., 277–292 (2005).

[5] Babilio, E. and Fortunato, A., "Numerical approximation of variational fracture through variable finite elements with gaps," In *Proc. AGS '08, Volume 1: Advanced Computations of Structures and Engineering Works*, 81-93. F. Darve, I. Doghri, R. El Fatmi, H. Hassis and H. Zenzri editors, G. Del Piero guest editor (2008).

[6] Angelillo, M., Babilio, E. and Fortunato, A., "A computational approach to quasi-static propagation of brittle fracture," In *Proc. Colloquium Lagrangianum 2002* (Lecture Notes in Applied and Computational Mechanics), Ravello (SA), Italy, November 6-9, 2002 (To appear).

[7] Angelillo, M., Babilio, E. and Fortunato, A., "A numerical approach to irreversible fracture as a free discontinuity problem," in *Proc. Colloquium Lagrangianum 2003* (Lecture Notes in Applied and Computational Mechanics), Montpellier, France, November 20–22 (To appear).

[8] Angelillo, M., Babilio, E., Cardamone, L. and Fortunato, A., "A numerical model for variational fracture based on discontinuous finite elements," In *Proc. 3rd CanCNSM*, Toronto, Canada, June 25–29, 2008, E. M. Croitoro ed. (To appear).

[9] Francfort, G. A. and Marigo, J. J., "Revisiting brittle fracture as an energy minimization problem," *J. Mech. Phys. Solids*, **46** (8), 1319-1342 (1998).

[10] Ambrosio, L., "Compactness theorem for a special class of functions of bounded variation," *Boll. Un. Mat. Ital.*, **3**–B, 857–881 (1989).

[11] Brakke, K. A., *Surface Evolver Manual*, Mathematics Department, Susquehanna University, Selinsgrove, (1999).

[12] Rice, J. R., "A path independent integral and the approximate analysis of strain concentration by notches and cracks," ASME*J. Appl. Mech.*, **35**, 379-386 (1968).

[13] Ma, L., Lu, T. J. and Korsunsky, A. M.,"Vector J–Integral analysis of crack interaction with pre–existing singularities". ASME *J. Appl. Mech.* **24**, 311–364. (1957).

[14] Irwin, G. R., "Analysis of stresses and strains near the end of a crack traversing a plate," ASME *J. Appl. Mech.* **73**, 876–883 (2006).

[15] Parks, D.M., "The virtual crack extension method for nonlinear material behavior," *Comp. Meth. Appl. Mech. Eng.*, **12**, 353–364 (1977).